NEW REINJECTION PROBABILITY FUNCTION FOR TYPE I, II AND III INTERMITTENCY

Sergio Elaskar[a] , Ezequiel del Rio[b] and José M. Donoso[b]

[a] *Departamento de Aeronáutica, Universidad Nacional de Córdoba and CONICET, Av. Vélez Sarfield 1611, Córdoba, Argentina, selaskar@efn.uncor.edu*

[b] *Escuela Técnica Superior de Ingenieros Aeronáuticos, Universidad Politécnica de Madrid, Plaza Cardenal Cisneros 3, Madrid, España, ezequiel.delrio@upm.es*

Abstract. There are several topics in fluid mechanics where the intermittency phenomenon appears, such as in Lorenz systems, Rayleigh-Bénard convection, DNLS equation and turbulence. The correct evaluation of the intermittency phenomenon contributes to a better prediction and a proper description of these topics. We summarized here a new method we have recently proposed to evaluate the reinjection probability function for type-II and type-III intermittencies. The new reinjection probability density (RPD) has been observed in the broad class of maps, as we have checked by both numerical simulations and analytical studies. For type-II and type-III intermittencies, we presented a new one-parameter family of functions describing the reinjection probability, being the usual type-II uniform reinjection probability a particular case of our RPD. For the type-III case, a new two-parameter family of RPD has been found from which one can derive the lower bound of reinjection (LBR). By extending the preceding analysis of type-II and type-III intermittencies, we give here a new RPD for the type-I case, from which we also derive the densities of the laminar phase lengths and the new characteristic relations.

Keywords: intermittency, chaos, reinjection

1 INTRODUCTION

Intermittency is a particular form of deterministic chaos, in which transition between laminar and chaotic phases occurs. A system is in regular behavior until, with a small change in a parameter, it begins to show chaotic burst at irregular intervals. Pomeau and Maneville introduced the intermittency concept in relation to the Lorenz system (Maneville and Pomeau, 1979; Pomeau and Maneville, 1980; Maneville, 1980). In this work we pay attention to this phenomenon since it is well-known that it emerges in several topics in the frame of the fluid mechanics, such as Lorenz system, Rayleigh-Bénard convection; derivative non-lineal Schoendinger equation and turbulence, among others.

The so-called intermittency phenomenon is classified into three types: I, II and III, according to the Floquet multipliers or eigenvalue in the local Poincaré map. For continuous-time system, the type-I intermittency arises in a cyclic-fold bifurcation, for which a stable and an unstable orbits collapse, therefore, the system loses the stable orbits in the vicinity of the vanished periodic orbits. For some maps, type-I intermittency occurs by means of an inverse tangent bifurcation, in this case an eigenvalue leaves the unit circle through +1. Intermittency type-II begins in a subcritical Hopf bifurcation, so that, two complex-conjugate Floquet multipliers or two complex-conjugate eigenvalues of the local Poincaré map exit in the unit circle. Intermittency of type-III is related to a subcritical period-doubling or flip bifurcation and one Floquet multiplier leaves the unit circle through -1.

In some previous papers, we have presented a new methodology to evaluate the main defining properties for type-II and type-III intermittencies, such as the reinjection probability density function (RPD), the probability density of the laminar phase, the average laminar length and the characteristic relation (del Río and Elaskar, 2009 and 2010; del Río, *et al.*, 2010; Elaskar and del Río, 2009; Elaskar *et al.*, 2010). In this work we extend this procedure to the type-I intermittency.

The local Poincaré maps for type-I, II and III intermittencies are usually written as

$$\begin{aligned} x_{n+1} &= \varepsilon + x_n + a\, x_n^2 \\ x_{n+1} &= (1+\varepsilon)\, x_n + a\, x_n^3 \qquad \text{with} \quad a > 0 \\ x_{n+1} &= -(1+\varepsilon)\, x_n - a\, x_n^3 \end{aligned} \tag{1}$$

for which the intermittency phenomenon exists only for $\varepsilon > 0$ (Rusbend, 1990; Shuster and Just, 2005; Kim *et al.*, 1997 and 1997a).

It is clear that the reinjection probability density $\phi(x)$, accounting with the transition from chaotic burst into the laminar zone, depends on each particular system or map making ϕ to be governed by the chaotic behavior of the system itself. The local Poincaré map of the intermittency does not give the necessary information to determine the reinjection probability density (RPD). In general, it is very difficult to obtain $\phi(x)$ analytically and it is also very complicated to set experimentally or numerically, because the large number of data needed to cover each interval of length δx in the reinjection region due to the noise introduced in numerical evaluations or in experimental measurements. Because of this, different approaches have been used in the literature to study the intermittent systems. The most usual and simple approximation considers $\phi(x)$ as a uniform function, not depending on the reinjection point (Shuster and Just, 2005). Many other approximations have been used, for instance, in type-Intermittency, Won and Kim (2000) assumed that the reinjection occurs in a fixed point Δ,

which gives $\phi(x) = \delta(x - \Delta)$. We refer here another interesting case where it was considered $\phi(x) \propto 1/\sqrt{x-\Delta}$ to study type-III intermittency in a electronic circuit (Won, *et al.* 2003).

Due to the disparity observed in modeling ϕ, we can conclude that it is very important to provide a method to obtain a correct form for the RPD for each different map, because once the RPD function is properly stated, it can be possible to describe some other characteristic parameters for the intermittency phenomenon. In the next section we present the new method to derive the RPD function for types I, II and III intermittencies by using numerical data. This technique can be also extrapolated to use the experimental data for the same purpose.

2 REINJECTION PROBABILITY DISTRIBUTION

In this paper, we do not directly measure the reinjection probability density $\phi(x)$ from the numerical data, instead of this, we numerically compute the function $M(x)$, defined as

$$M(x) = \frac{\int_{x_i}^{x} \tau\, \phi(\tau)\, d\tau}{\int_{x_i}^{x} \phi(\tau)\, d\tau} \quad if \quad \phi(\tau) \neq 0; \qquad M(x) = 0 \quad if \quad \phi(\tau) = 0 \tag{2}$$

where x_i is the closed point to the unstable fixed point where the reinjection takes place, *i.e.* it is the lower bound of the reinjection. The integration interval $[x_i\ ,\ c]$ defines the laminar region. $M(x)$ has been calculated for a broad class of maps numerically, and it has been stated that if exhibits the linear form

$$M(x) = m\, x + x_h \tag{3}$$

as a very good approximation. This form generalizes the function introduced by del Río and Elaskar (2009). From Eq.(2) it possible to determine that $M(x_i) = x_i$, then, it verifies

$$M(x) = m\left(x - x_i\right) + x_i \tag{4}$$

where the slope m plays an important role in the intermittency dynamics. Therefore, the function $M(x)$ has been proved to be an useful tool to study type-II and type-III intermittencies. From Eq.(4) and Eq.(2) the reinjection probability density can be deduced, giving

$$\phi(x) = \Lambda\left(x - x_i\right)^{\alpha} \quad with \quad \alpha = \frac{1-2m}{m-1}, \tag{5}$$

where Λ is the normalization constant, which can be written as

$$\Lambda = k\,\frac{\alpha+1}{\left(c - x_i\right)^{\alpha+1}} = k\,\frac{m}{1-m}\left(c - x_i\right)^{m/(m-1)} \tag{6}$$

with $k = 1$ and $k = 0.5$ for type-II and type-III intermittencies, respectively. Note that the slope m must satisfy the condition $0 < m < 1$ which has been met in all our numerical tests. The

usual uniform probability reinjection is recovered for $m = 0.5$ with $x_i = 0$, leading to $M(x) = 0.5\,x$.

3 INTEMITTENCY TYPE-I

The new technique is now applied to study the type-I intermittency using the illustrating map

$$\begin{aligned} x_{n+1} &= \varepsilon + x_n + a\,x_n^2 \qquad if \qquad x_n \le x_l \\ x_{n+1} &= \left(\frac{x - x_l}{1 - x_l}\right)^s \qquad if \qquad x_n \le x_l \end{aligned} \tag{7}$$

where x_l is such that $\varepsilon + x_l + a\,x_l^2 = 1$. For $\varepsilon = 0$ the origin is a fixed point, however, for $\varepsilon > 0$ all points x close to the origin move away in a process driven by the parameters ε and a. When the n-th iterated value x_n approaches x_l the reinjection mechanism starts, governed by exponent s. Figure 1 shows the map (7) for $s = 0.5$, 1 and 2 for the black, red and purple lines respectively, and Figure 2 shows the map time evolution of the laminar and chaotic behaviors with irregular lasting. Figure 3 depicts the bifurcation diagram to illustrate the instability at $\varepsilon=0$, for $a = 1$, $s = 2$.

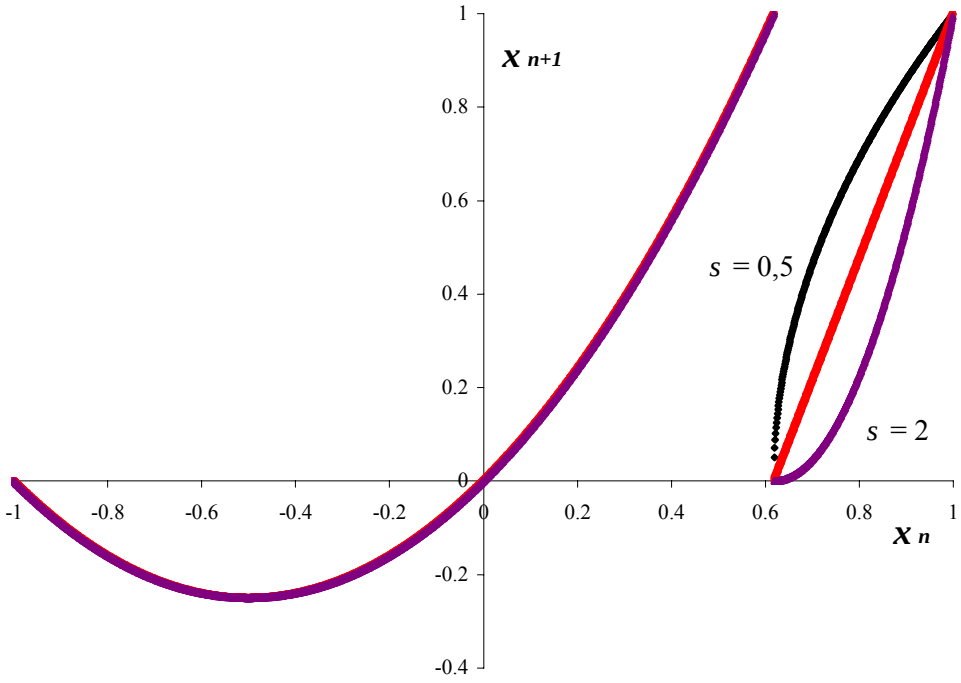

Figure 1. Map (7) with $\varepsilon = 0.000001$ for $s = 0.5$ (in black), for $s = 1$ (red) and $s = 2$ (purple).

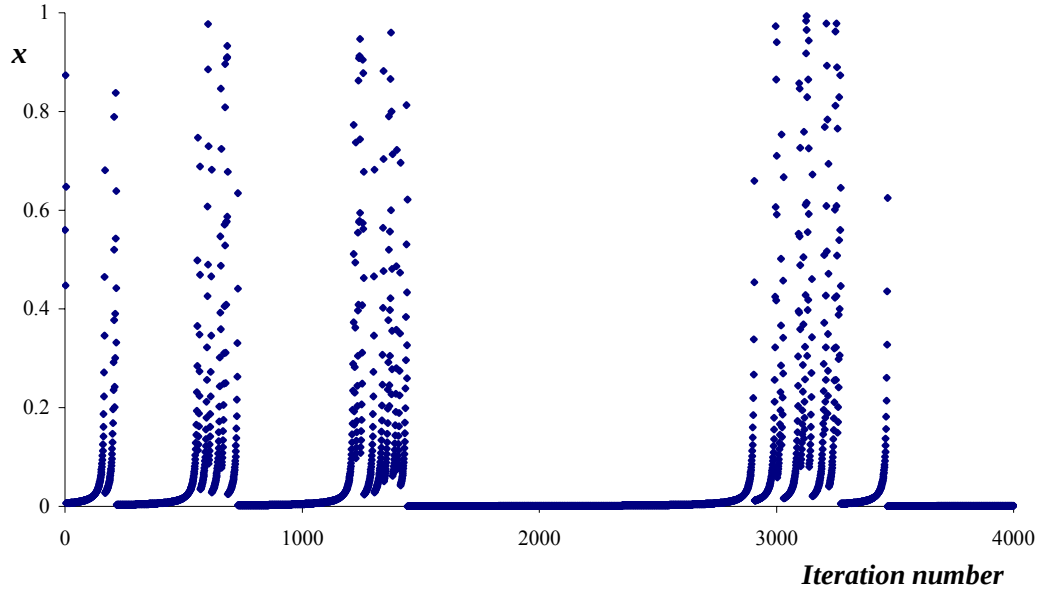

Figure 2. Eq.(7) map time evolution for $\varepsilon = 0.000001$, $a = 1$, $s = 2$.

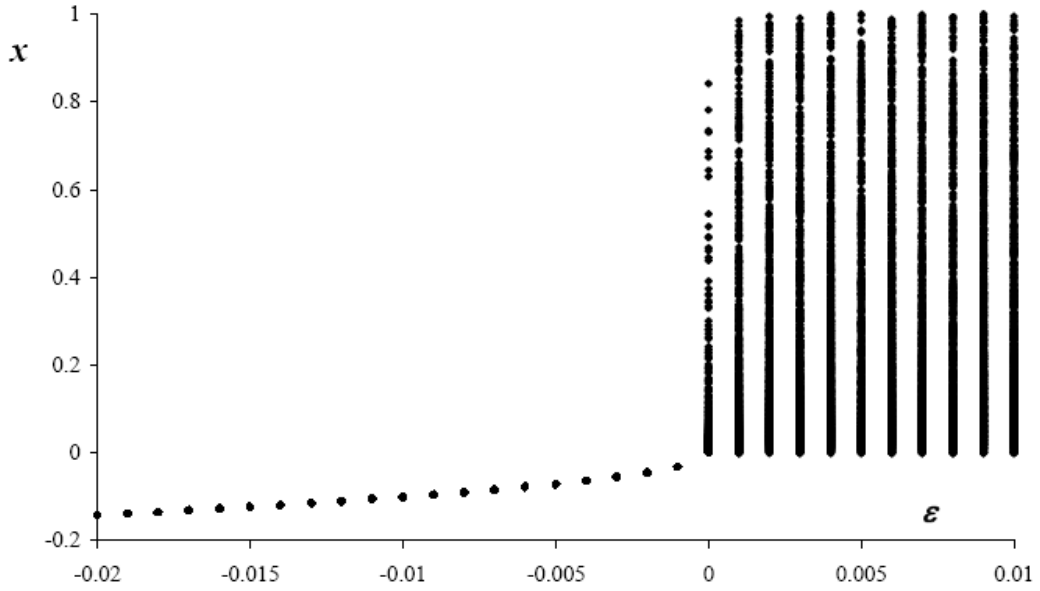

Figure 3. Bifurcation diagram for Eq.(3). $s = 2$ and $a = 1$.

3.1 Reinjection probability density function

In this section we compute the RPD by using $M(x)$ computed after having carried out several numerical tests. The results are presented in Fig. 4, where the three straight lines, crossing the origin, $x_i = 0$ in Eq.(4), correspond to the indicated values of s.

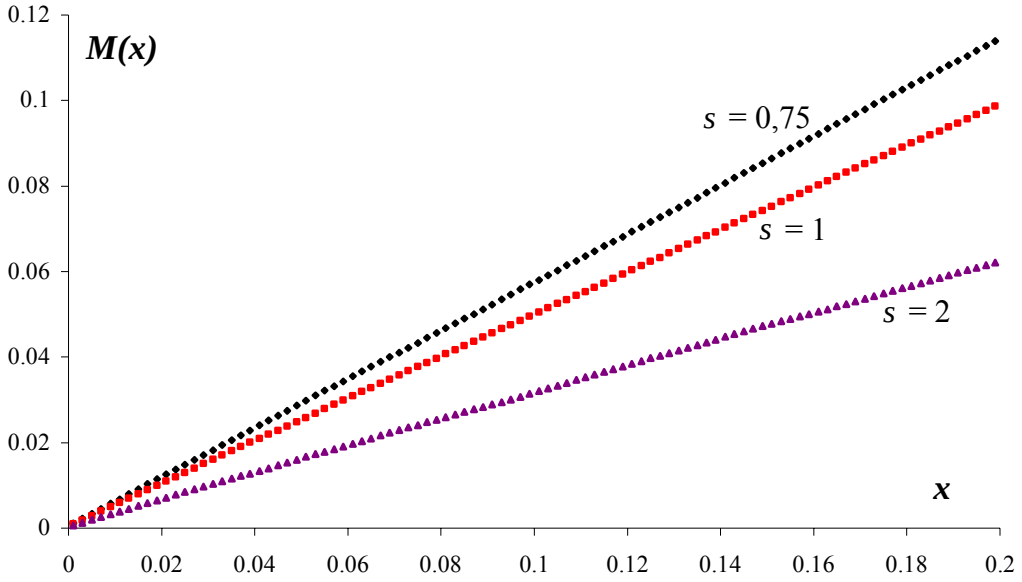

Figure 4. Function M(x). s = 0.75; 1 and 2; a = 1 and ε = 0.000001.

After applying the least square method, we have obtained the corresponding m values of the M slope and each exponent α appearing in Eq.(5), as follows

$s = 0.75,$ $m = 0.5686$ $\alpha = 0.318$
$s = 1.0,$ $m = 0.4936 \approx 0.5$ $\alpha = -0.02516 \approx 0$
$s = 2.0,$ $m = 0.3104$ $\alpha = -0.55$

In this kind of intermittency, $k=1$, the RPD normalization reads

$$\int_0^c \phi(x)\, dx = \int_0^c \Lambda\, x^{\alpha} dx = 1, \tag{8}$$

which convergences for $\alpha > -1$, giving for Λ the expression

$$\Lambda = \frac{\alpha+1}{c^{\alpha+1}} = \frac{m}{1-m}\, c^{m/(m-1)} \tag{9}$$

and the RPD for type-I intermittency is finally given by

$$\phi(x) = \frac{m}{1-m}\, c^{m/(m-1)}\, x^{\frac{1-2m}{m-1}} = \frac{\alpha+1}{c^{\alpha+1}}\, x^{\alpha} \tag{10}$$

only depending on m. The comparison between the RPD obtained numerically with the analytical RPD calculated by means of Eq.(10) is depicted in Figures 5a, b and c, where, as in the remaining plots in this paper, dots stand for the numerical results and the solid lines correspond to analytical expressions. In these figures it can be checked out how the theoretical RDP properly assembles the numerical RPD for the three test cases, each one having a characteristic distinguishable non-linear (global) behavior, in particular, the RPD is

approximately constant in Fig 5b since α is close to zero.

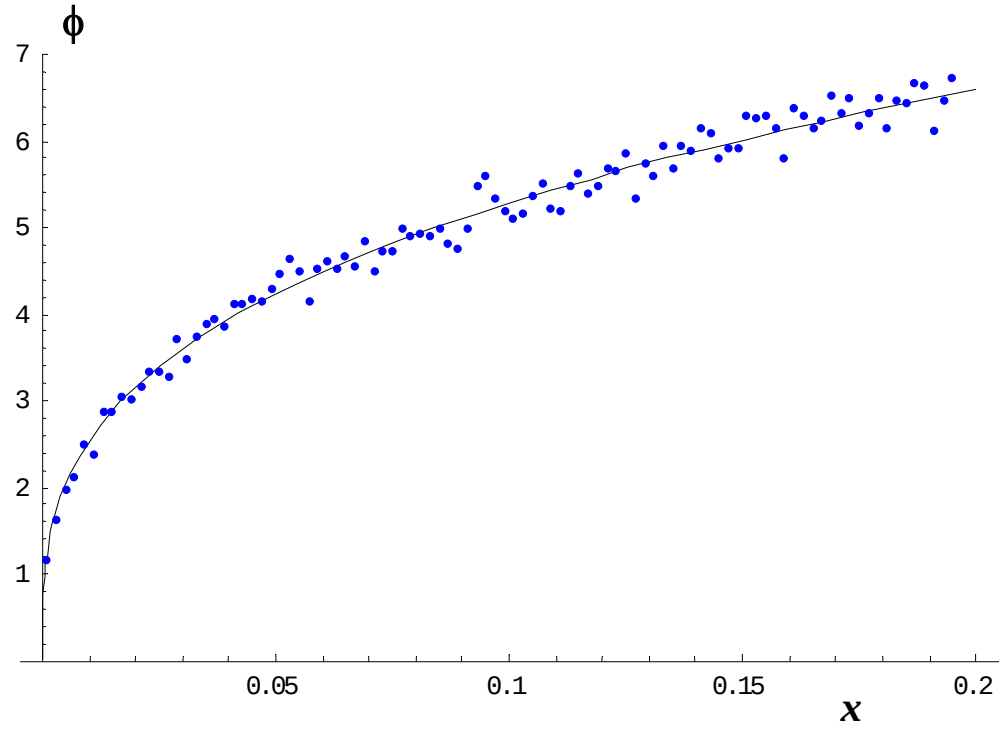

Figure 5a. The RPD as a function of x for $s = 0.75$, $\varepsilon = 0.00001$, $c = 0.2$. Dots stand for numerical results and the solid line plots the function given by Eq.(10)

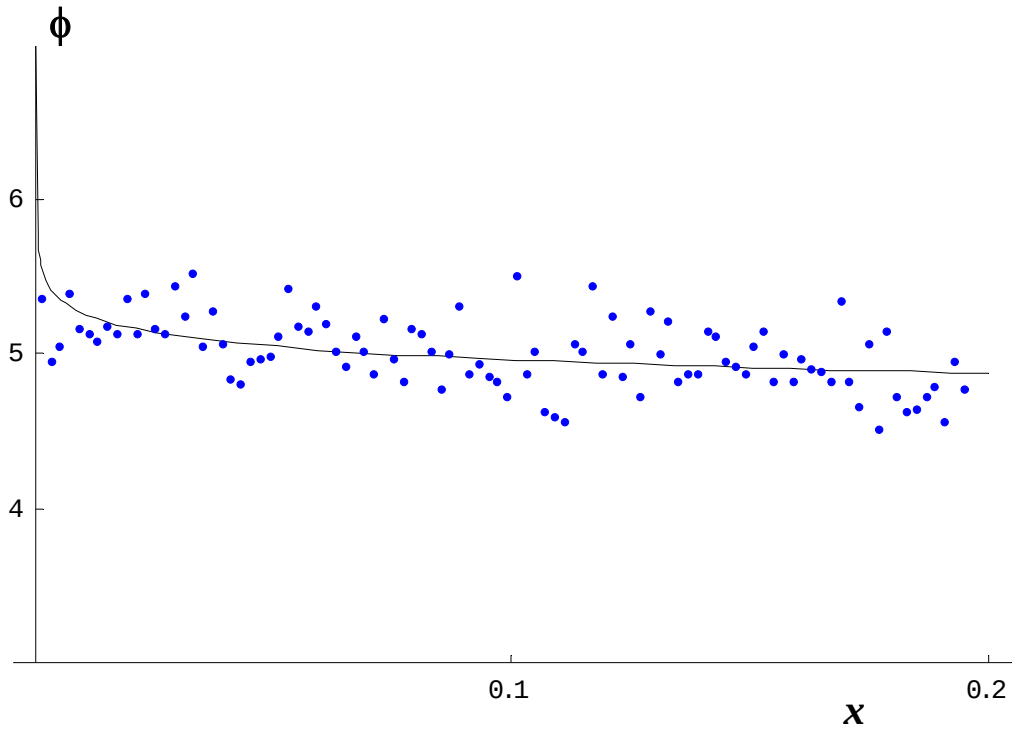

Figure 5b. The RPD for $s = 1$, $\varepsilon = 0.00001$, $c = 0.2$.

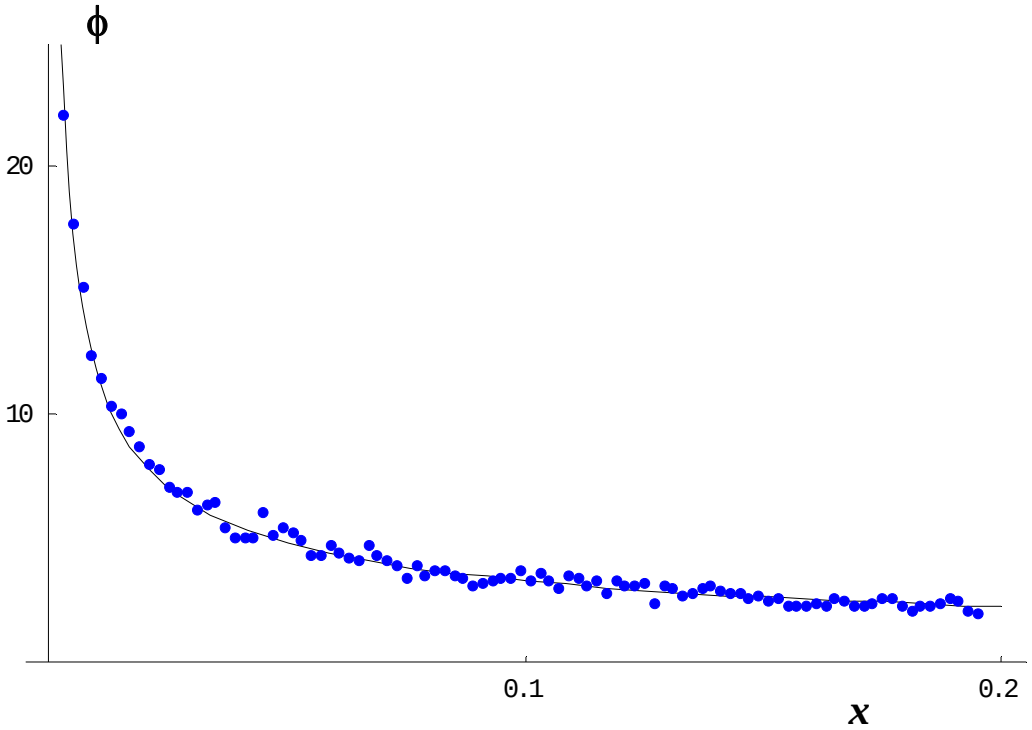

Figure 5c. The RPD for s = 2, , ε = 0.00001, c = 0.2.

3.2 Probability of the laminar length

Another important parameter for studying the intermittency phenomenon is the probability associated to the laminar length variable giving the probability of having a laminar length between l and $l+dl$. Following the usual method based on interpretation transposing the map local difference equation into a continuous differential equation inside the laminar region (Shuster and Just, 2005), for type-I intermittency, Eq.(1), we have

$$\frac{dx}{dl} = \varepsilon + a\, x^2 \tag{11}$$

where l counts the number of iterations in the laminar region. After integration of the Eq.(11) we have

$$l(x,c) = \frac{1}{\sqrt{a\varepsilon}}\left[\arctan\left(c\frac{\sqrt{a}}{\sqrt{\varepsilon}}\right) - \arctan\left(x\frac{\sqrt{a}}{\sqrt{\varepsilon}}\right)\right] \tag{12}$$

which clearly evidences that the laminar iteration number (length of the laminar region) only depends on the local map but not on the global one. Finally, the probability of finding a laminar phase length inside the interval (l; l+dl) , $\phi_l(l)$, is given by

$$\phi_l(l) = \phi(X(l,c))\left|\frac{dX(l,c)}{dl}\right| \tag{13}$$

where $X(l,c)$ is the inverse of the $l(x,c)$ (with respect to x) extracted from Eq.(12) as

$$X(l,c)=\frac{\sqrt{\varepsilon}}{\sqrt{a}}\tan\left[\arctan\left(c\frac{\sqrt{a}}{\sqrt{\varepsilon}}\right)-l\sqrt{a\varepsilon}\right]. \tag{14}$$

After substituting Eq.(14) into Eq.(13) the required probability is

$$\phi_l(l)=\frac{\varepsilon^{1+\alpha/2}}{a^{\alpha/2}}\Lambda\ \sec^2(z)\tan^{\alpha}(z);\qquad z=\arctan\left(c\frac{\sqrt{a}}{\sqrt{\varepsilon}}\right)-l\sqrt{a\varepsilon} \tag{15}$$

which for when $l\to 0$, behaves as

$$\lim_{l\to 0}\phi_l(l)\to\Lambda c^{\alpha}\left(\varepsilon+a c^2\right) \tag{16}$$

This last equation indicates that for a very small ε, $\phi_l(0)$ is approximately constant and independent of ε,

$$\phi_l(0)\approx a c^{2+\alpha}\Lambda \tag{17}$$

For any positive α, the function $\phi_l(l)$ is a decreasing function of l, being $\phi_l(l)=0$ when l equals the value

$$l_m=\frac{\arctan\left(c\frac{\sqrt{a}}{\sqrt{\varepsilon}}\right)}{\sqrt{a\varepsilon}} \tag{18}$$

for $\alpha<0$, however, Eq.(18) determines the maximum laminar phase length and for $l=l_m$ the probability of the laminar length satisfies

$$\lim_{l\to l_m}\phi_l(l)\to\infty, \tag{19}$$

meaning that for negative α values, the laminar length $l=l_m$ is a cut-off. Having in mind the previous relations, we can conclude that there always exists a limit value l_m for l, meanwhile the behavior of $\phi_l(l)$ depends on the sign of α since for $\alpha\le 0$, $\lim_{l\to l_m}\phi_l(l)\to\infty$ and for $\alpha>0$ $\lim_{l\to l_m}\phi_l(l)\to 0$.

In general, the behavior of $\phi_l(l)$ is determined by Eq.(15) and see two relevant cases can be usefully distinguished. For $\alpha\neq 0$ two factors govern Eq.(15), $\sec^2(z)$ and $\tan^{\alpha}(z)$, the former is always positive whereas $\tan^{\alpha}(0)=0$, furthermore, for $z=0$, a limit value $l=l_m$, exists for $\alpha<0$ giving $\lim_{l\to l_m}\phi_l(l)\to\infty$ and for $\alpha>0$, $\lim_{l\to l_m}\phi_l(l)\to 0$. For $\alpha=0$, the factor $\tan(z)$ disappears and $\phi_l(l)$ is only depending on the factor $\sec^2(z)$, *i.e.* $\lim_{l\to l_m}\phi_l(l)\to\infty$,

however in this case $l = l_m$ when $z = \pi/2$

$$l_m = \frac{\arctan\left(c\frac{\sqrt{a}}{\sqrt{\varepsilon}}\right) - \frac{\pi}{2}}{\sqrt{a\varepsilon}}$$

which combined with Eq.(18) gives $\lim_{\varepsilon \to 0} l_m \to \infty$.

The figure Fig. 6 displays the characteristic behavior $\phi_l(l)$ for positive α. Here, $s = 0.6$ ($\alpha \simeq 0.665$) for both numerical (dots) and analytical results, with Eq.(15). By means of Eq.(17) we obtain $\phi_l(0) \simeq 0.16$ and from Eq.(18) we have $l_m = 147$. In a similar way, in Fig. 7 the typical $\phi_l(l)$ behavior for negative α is presented. An excellent agreement between numerical and Eq.(15, 17 and 18) analytical results has been found again in all tested cases.

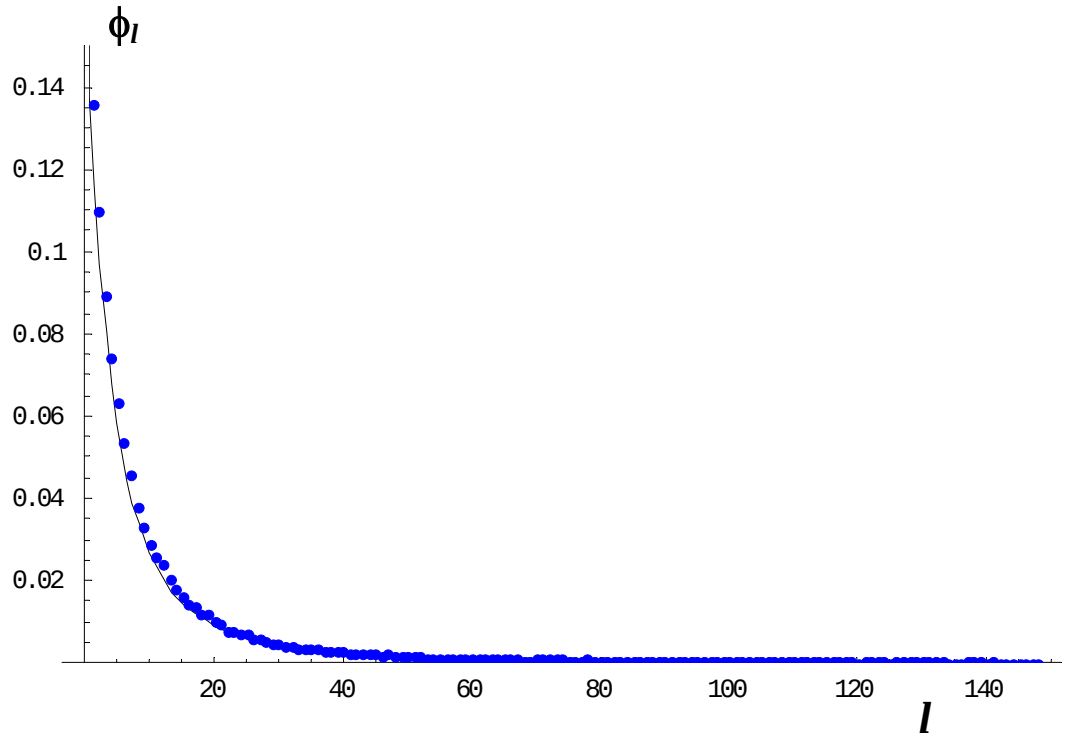

Figure 6. The probability of the laminar length for $s = 0.6$, $\varepsilon = 0.0001$, $\alpha \simeq -0.665$, $c = 0.1$. The solid line is obtained from Eq.(15).

3.3 Characteristic relation

The dependence of the average length of a laminar region on ε is denominated the characteristic relation. The average length L can be obtained as:

$$L = \int_{x_i}^{c} \phi(x)\, l(x,c)\, dx \qquad (20)$$

with the definition of the $\phi(x)$ in Eq.(10), we get:

$$L = \int_{x_i}^{c} \left\{ \frac{m\, c^{m/(m-1)}}{1-m} \; \frac{x^{\frac{1-2m}{m-1}}}{\sqrt{a\varepsilon}} \left[\arctan\left(c\frac{\sqrt{a}}{\sqrt{\varepsilon}} \right) - \arctan\left(x\frac{\sqrt{a}}{\sqrt{\varepsilon}} \right) \right] \right\} dx \tag{21}$$

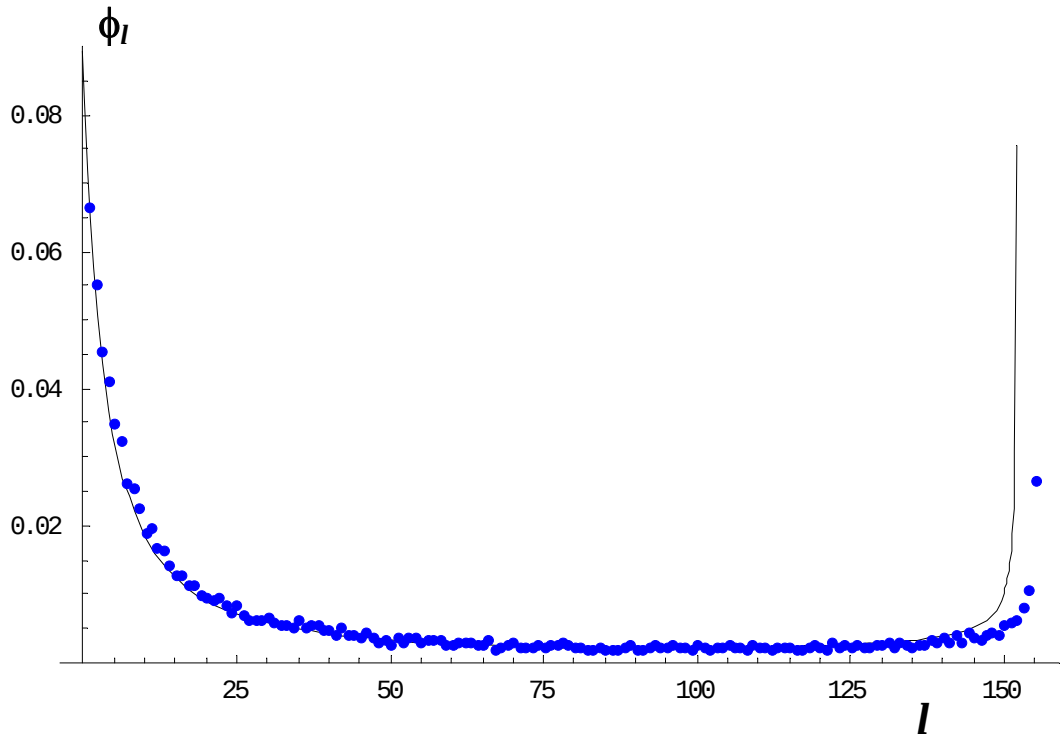

Figure 7. The probability of the laminar length for $s = 2$, $\varepsilon = 0{,}0001$, $\alpha \simeq -0{,}555$, $c = 0.2$.

To solve the integral (21), we can decompose it into two parts (here $a = 1$ and $x_i = 0$)

$$\begin{aligned} L &= \frac{m\, c^{m/(m-1)}}{(1-m)\sqrt{\varepsilon}} \left(I_1 - I_2 \right) = k\left(I_1 - I_2 \right); \qquad k = \frac{\Lambda}{\sqrt{\varepsilon}} \\ L &= k\left[\int_0^c x^{\alpha} \arctan\left(\frac{c}{\sqrt{\varepsilon}} \right) dx - \int_0^c x^{\alpha} \arctan\left(\frac{x}{\sqrt{\varepsilon}} \right) dx \right] \end{aligned} \tag{22}$$

The solution of the first integral is directly given by

$$I_1 = \frac{c^{\alpha+1}}{\alpha+1} \arctan\left(\frac{c}{\sqrt{\varepsilon}} \right) \tag{23}$$

and I_2 can be integrated by parts with

$$u = \arctan\left(\frac{x}{\sqrt{\varepsilon}}\right) \qquad v = \frac{x^{\alpha+1}}{\alpha+1} \tag{24}$$

so that

$$\begin{aligned} I_2 &= \arctan\left(\frac{c}{\sqrt{\varepsilon}}\right)\frac{c^{\alpha+1}}{\alpha+1} - \frac{\sqrt{\varepsilon}}{\alpha+1}\int_0^c \frac{x^{\alpha+1}}{\varepsilon + x^2}\,dx \\ I_2 &= \arctan\left(\frac{c}{\sqrt{\varepsilon}}\right)\frac{c^{\alpha+1}}{\alpha+1} - \frac{\sqrt{\varepsilon}}{\alpha+1} I_3 \end{aligned} \tag{25}$$

If we replace the expressions for I_1 and I_2 in the L definition, we have:

$$L = k\frac{\sqrt{\varepsilon}}{\alpha+1} I_3 = \frac{1}{c^{\alpha+1}} I_3 = \frac{1}{c^{\alpha+1}}\int_0^c \frac{x^{\alpha+1}}{\varepsilon + x^2}\,dx \tag{26}$$

now, taking $x = y\sqrt{\varepsilon}$, the integral I_3 can be written as

$$I_3 = \varepsilon^{\alpha/2}\int_0^{\frac{c}{\sqrt{\varepsilon}}} \frac{y^{\alpha+1}}{\left(1+y^2\right)}\,dy = \varepsilon^{\alpha/2}\int_0^{\infty} \frac{y^{\alpha+1}}{\left(1+y^2\right)}\,dy - \varepsilon^{\alpha/2}\int_{\frac{c}{\sqrt{\varepsilon}}}^{\infty} \frac{y^{\alpha+1}}{\left(1+y^2\right)}\,dy \tag{27}$$

The second integral goes to zero as ε goes to zero, the first integral converges if α is greater than -2 and less than 0, and the average laminar length is finale given by

$$L = \frac{\pi\,\varepsilon^{\frac{\alpha}{2}}}{c^{\alpha+1}\sec\left(\frac{\pi\alpha}{2}\right)} \quad \Rightarrow \quad L \propto \varepsilon^{\frac{\alpha}{2}} \tag{28}$$

In the previous calculation we have assumed α as independent of the very small parameter ε, as observed in the numerical experiments. In the Figure 8 it is shown the characteristic relation for α = -0.376 (s = 1.5) and α = -0.555 (s = 2). The numerical values (dots) are presented by the straight lines obtained by least square fitting. It can be checked that each line slope is in agreement with the value α/2 predicted by Eq.(28), as presented in following table

s	α/2	Slope in Figure 8
1.5	-0.183	-0.178
2	-0.27	-0.257

Table 1. Comparison between numerical and theoretical slopes from Fig. 8 and Eq.(28)

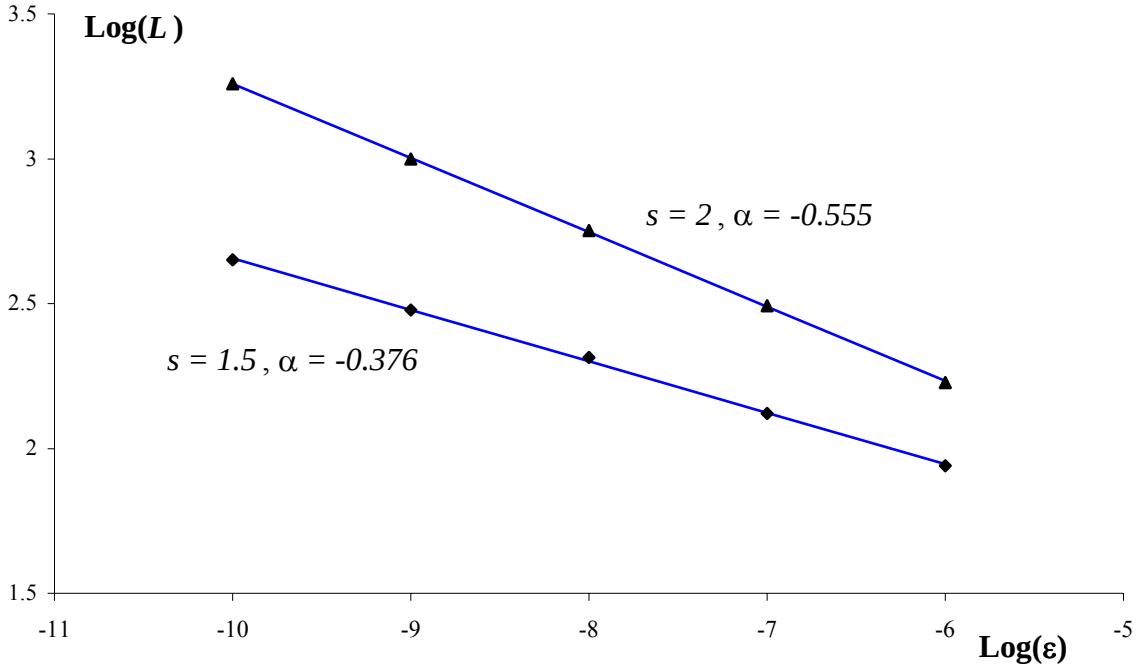

Figure 8. Characteristic relation. Marks stand for numerical data and lines correspond to least square fitting.

For the uniform reinjection as a particular case, $\alpha = 0$, the integral I_3 reads

$$L = \frac{1}{c} I_3 = \frac{1}{c} \int_0^c \frac{x}{\varepsilon + x^2} dx = \frac{0.5}{c} \ln\left(\frac{c^2}{\varepsilon} + 1\right) = 0.5\, \Lambda \ln\left(\frac{c^2}{\varepsilon} + 1\right) \tag{29}$$

and for small ε we have

$$L \approx \frac{0.5}{c}\left[\ln\left(c^2\right) - \ln\left(\varepsilon\right)\right] \propto -\ln\left(\varepsilon\right) \tag{30}$$

providing, as expected, the classical form of the characteristic relation, Kim *et al.* (1994) and Cho *et al.* (2002), this behavior can be seen in Figure 9 obtained for $s = 1$ and $\alpha \simeq -0.03$.

For the case of positive α, we have to numerically compute L by using Eq. (21). The results are presented in Figures 10 and 11, showing a good correspondence between the numerical and theoretical results.

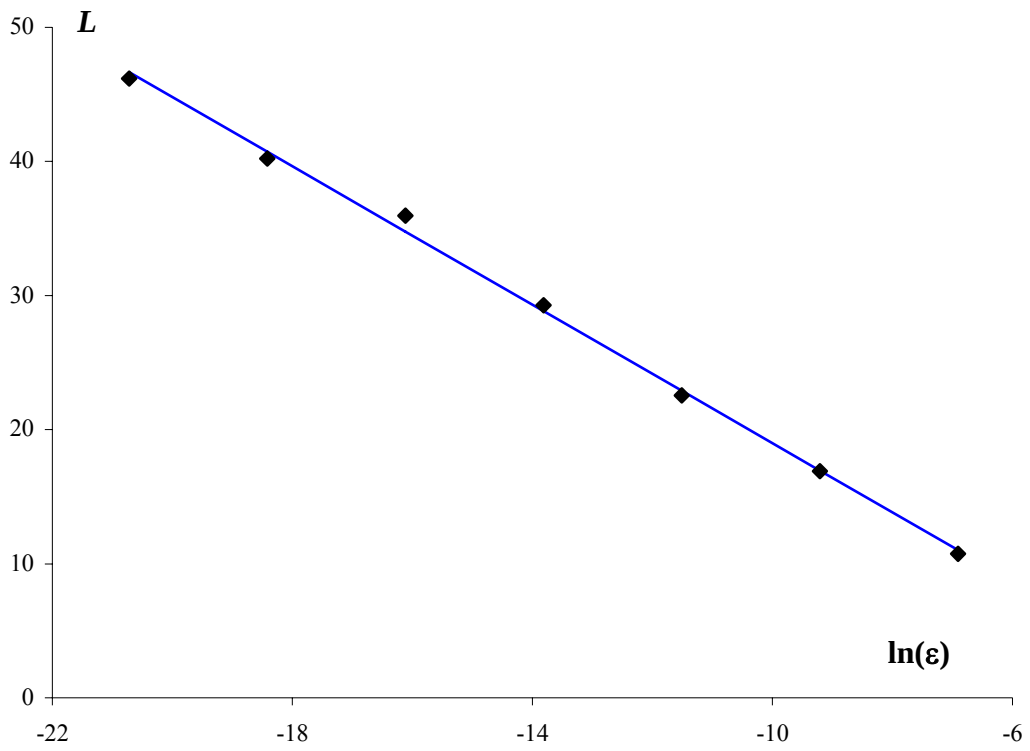

Figure 9. Characteristic relation for $\alpha = 0$.

3.4 The Liapunov exponent

For any map $x_{n+1} = f(x_n)$, the Liapunov exponent $\lambda(x)$, is defined as

$$\lambda(x) = \lim_{N\to\infty}\lim_{\delta\to 0} \frac{1}{N}\log\frac{f^N(x+\delta)-f^N(x)}{\delta} = \lim_{N\to\infty}\frac{1}{N}\log\frac{d\, f^N(x)}{d(x)} \tag{31}$$

where N is the number of iterations. Eq. (31) indicates that $e^{\lambda(x)}$ is the average factor by which the distance between closely adjacent points becomes stretched after one iteration (Schuster and Just, 2005), $(\delta x)_N = (\delta x)_0\, e^{\lambda N}$. The relation $1/\lambda$ is called the Liapunov time and systems showing an exponential divergence, a positive λ, are referred as chaotic systems characterized by and an intrinsic scale defined by the Liapunov time. After a long time evolution with respect to the Liapunov time, these systems lose the initial state information (Prigogine, 2009).

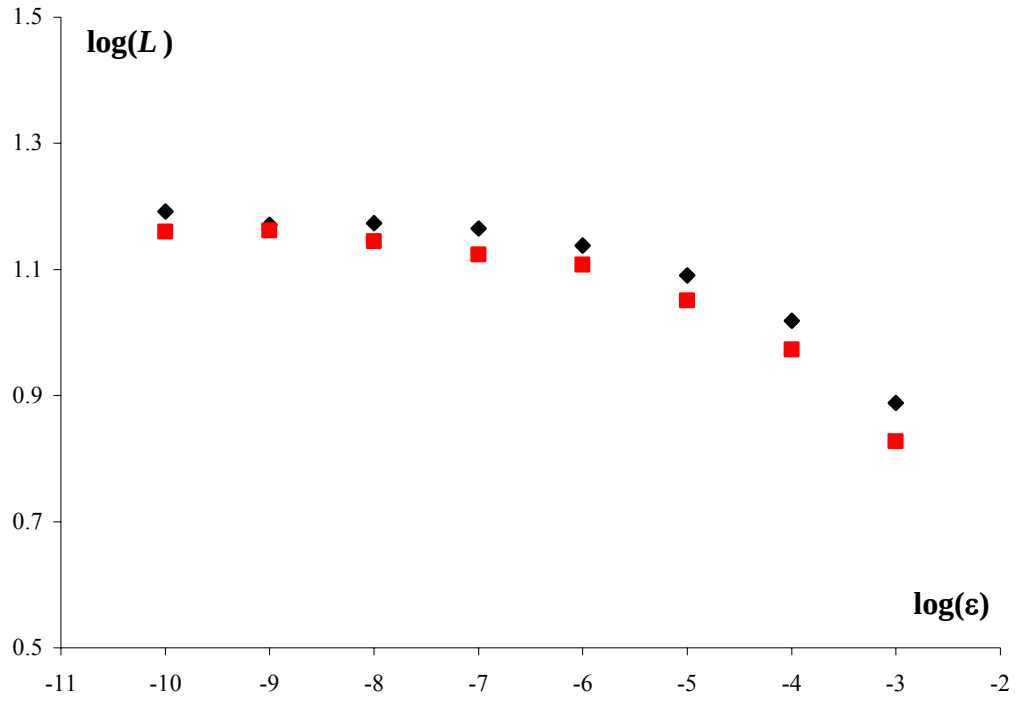

Figure 10. Characteristic relation for $s = 0.75$, $\alpha = 0.328$. Blue marks stand for numerical results and the red ones correspond to values obtained after numerical integration of Eq.(21).

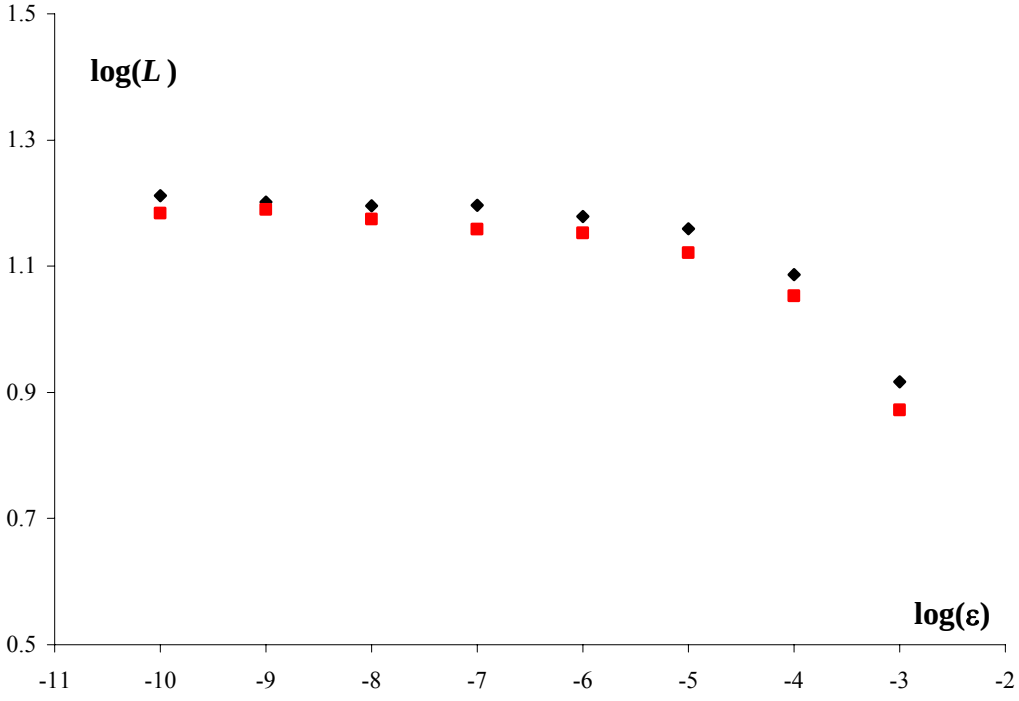

Figure 11. Characteristic relation for $s = 0.6$, $\alpha = 0.665$. Blue marks stand for numerical results and the red ones correspond to values obtained after numerical integration of Eq.(21).

It is interesting to note here that log(λ) is a linear function of log(ε), as shown in Fig. 12 for s = 1,5 and s=2, so that we can write $\lambda \propto \varepsilon^{\sigma}$. By least square method, we have checked that the relation $\sigma \approx -\alpha/2$ holds, however, this topic demands further investigations.

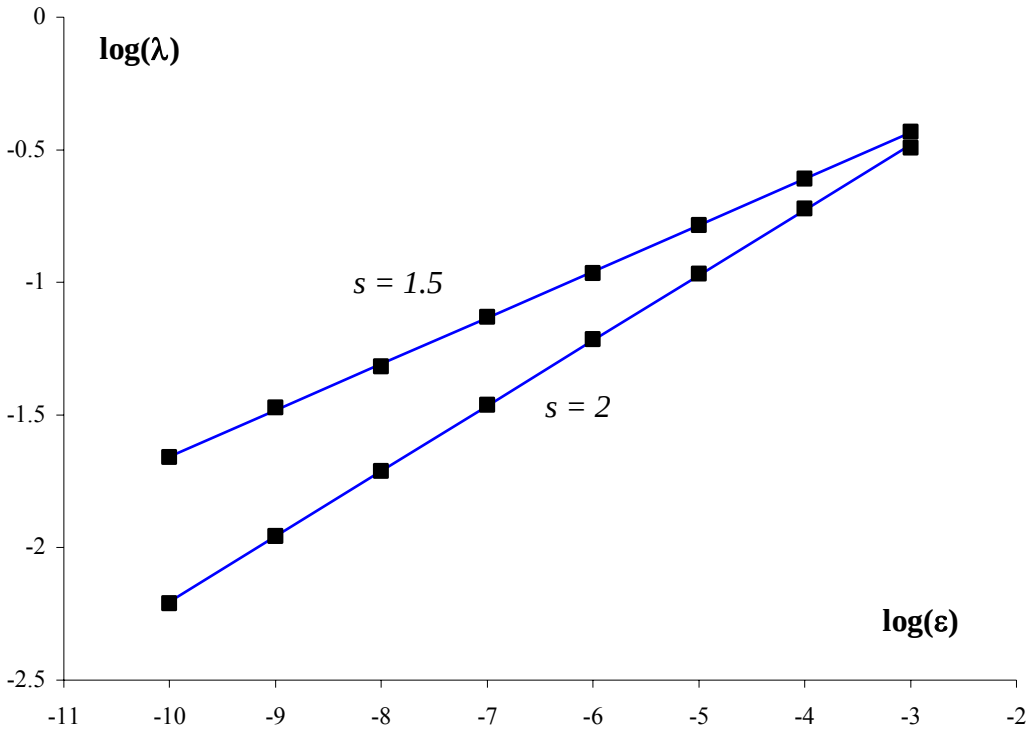

Figure 12. Liapunov exponent.

3.5 Relation between α and s

As shown in a previous paper (del Río and Elaskar, 2009) a relation exists between the coefficient α and the exponent s (s=q in that work)

$$\alpha = \frac{1}{s} - 1 \tag{32}$$

which holds in our case for the map Eq.(7), as can be seen in Figure 13.

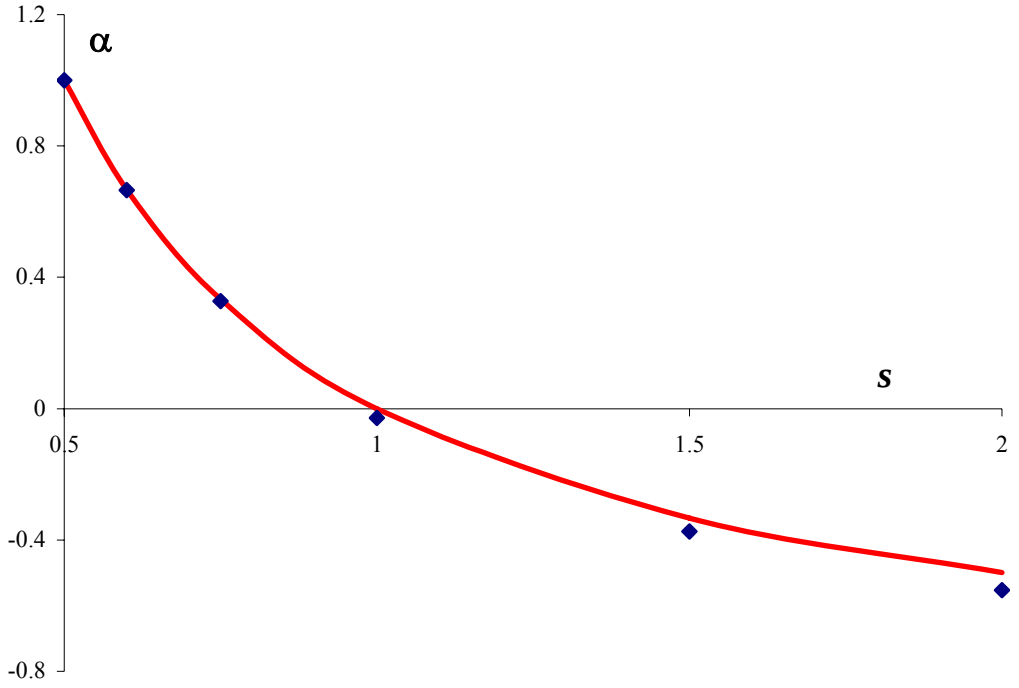

Figure 13. Relation between α and the exponent *s*. Marks stand for numerical results and the solid line corresponds to Eq.(32).

4 LOGISTIC MAP

Kim, *et al.* (1994) analyzed the following logistic map:

$$F(A,B,x) = f^{A}[f^{B}(x)]; \quad f^{A}(x) = 4Ax(1-x); \quad f^{B}(x) = 4Bx(1-x) \tag{33}$$

For the previous equations, type-I intermittency occurs for:

$$\begin{aligned} x_c &= \frac{2}{3} - \frac{\sqrt{4-3/B_c}}{6} \\ B_c &= \frac{-9A^{0.5} + 8A^{1.5} + (4A-3)^{1.5}}{16A^{0.5}(A-1)} \end{aligned} \tag{34}$$

The intermittent phenomenon presents a lower bound of reinjection (LBR). The LBR is a function of A and can be negative, zero or positive. Kim *et al.* (1994) found that the reinjection probability density function possesses the form:

$$\phi(x) \propto \left(x - x_L\right)^{-0.5} \tag{35}$$

where x_L is the LBR. We note that the Eq.(35) is a particular case of the Eq.(5) with $\alpha = -0.5$ or $m = 1/3$.

We carried out several numerical tests, using Eqs.(2-4), to evaluate the function $M(x)$ and the slope m. In all numerical tests we obtained that $m \cong 1/3$ independently of the LBR value. As

examples we show in Figures 14 and 15 the RPD as function of the laminar interval, blue points represent the numerical evaluations and continuous lines indicate the theoretical predictions. Figure 14 corresponds to $A = 0.94146194$; $B_c = 0.830195$; $x_c = 0.563066$; $\varepsilon = 0.0001$ and the laminar interval is $c = 0.01$. Figure 15 exhibits the results for $A = 0.9415$; $B_c = 0.830205$; $x_c = 0.56306$; $\varepsilon = 0.000001$ and $c = 0.02$. From the two pictures we can observe a very good correspondence between the numerical dates and the theoretical values.

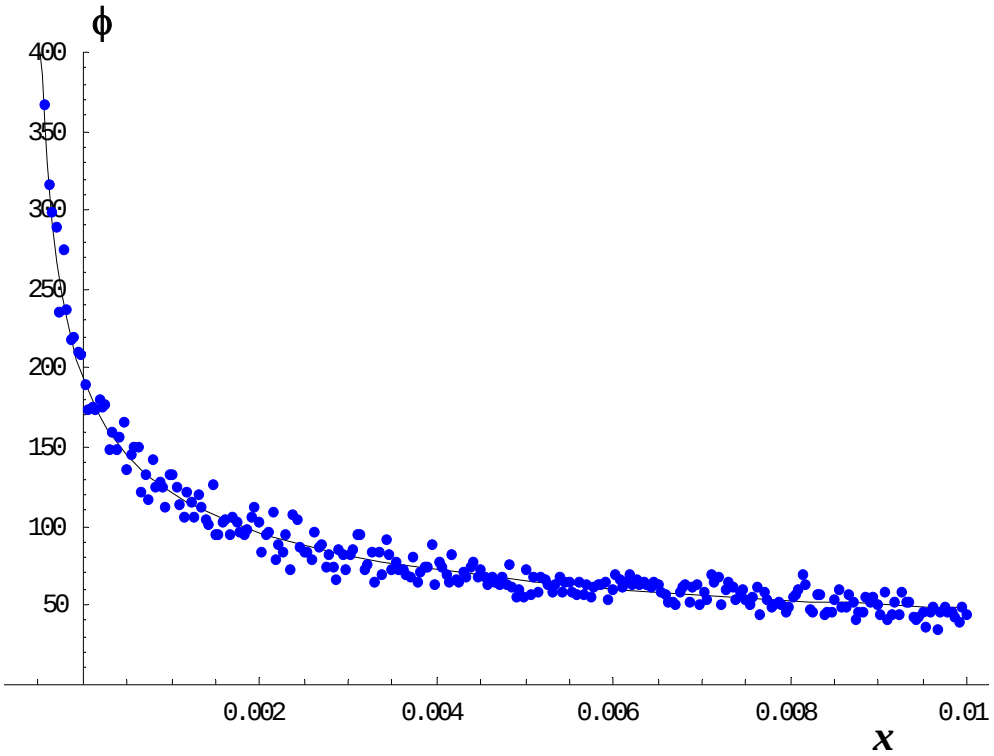

Figure 14. Reinjection probability function for logistic map given by Eq.(33). $A = 0.94146194$; $B_c = 0.830195$; $x_c = 0.563066$; $\varepsilon = 0.0001$ and $c = 0.01$

Eq.(33) and Eq.(7) define a very different functions, however both maps posses type-I intermittency and in both maps the intermittency phenomenon has the same exponential form for the reinjection probability density function. On the other hand, the function $M(x)$ has shown to be an accurate tool to evaluate the reinjection probability density function.

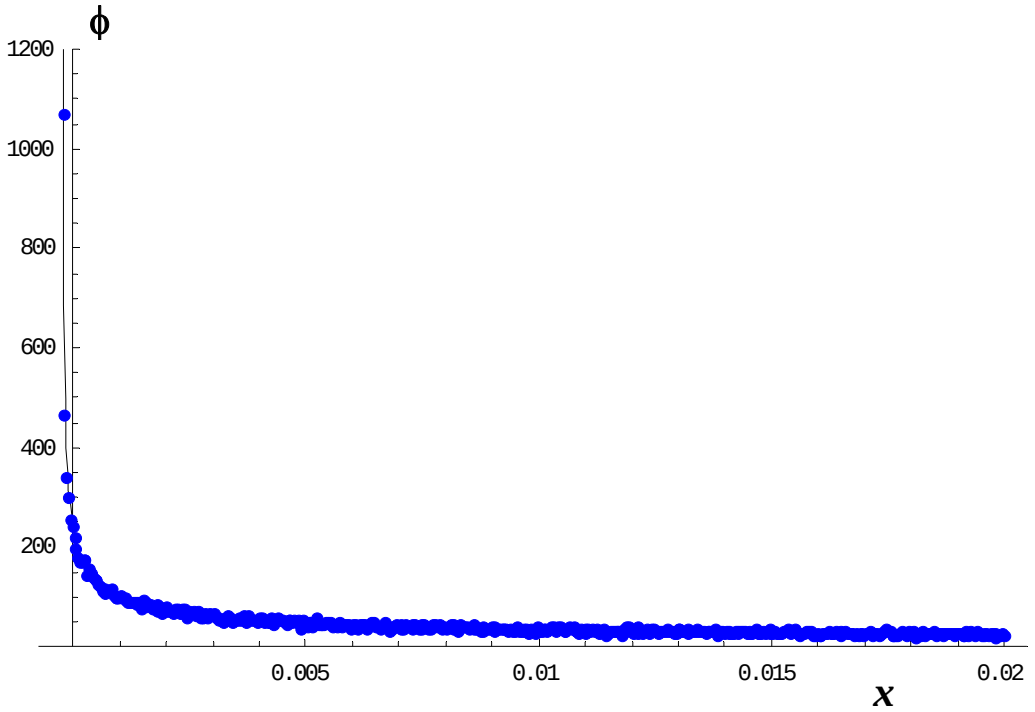

Figure 15. Reinjection probability function for logistic map given by Eq.(33). $A = 0.9415$; $B_c = 0.830205$; $x_c = 0.56306$; $\varepsilon = 0.000001$ and $c = 0.02$.

5 CONCLUSIONS

In this paper we have extended to the type-I intermittency phenomenon the analysis procedure we developed in a previous work in studying type-II and type-III intermittencies. We have found that our function $M(x)$ is also a key tool to analyze the type-I intermittency, especially when numerical or experimental data are required in the investigation, since it is easily obtained. Therefore, $M(x)$ is more useful and simpler than the reinjection probability density ϕ which can be derived form the former. As a matter of fact, the reinjection probability density function, the probability of the laminar length, the average laminar length and the characteristic relation have been obtained for this case by means of numerical computations finding a good agreement with theoretical predictions. In all numerical tests we have obtained that $M(x)$ is linear, $M(x) = m\,x$, and we have found a power law for the RPD as $\phi(x) = \lambda\, x^{\alpha}$ which extended the usual uniform RPD, a particular case of ours for $\alpha = 0$ or $m = ½$. We have also verified that the relation between s and α, Eq.(32), deduced for a broad class of maps, properly holds for type-I intermittency.

Acknowledgements. This paper was supported by grants PIP - No 11220090100809 of CONICET, Universidad Politécnica de Madrid, Universidad Nacional de Córdoba, Ministerio de Ciencia y Tecnología de Córdoba and Ministerio de Ciencia de España under projects ENE2007-67406-C02-01, AYA2008-04769.

REFERENCES

Cho, J.; Ko, M.; Park, Y. and Kim, C., Experimental observation of the characteristic relations of type-I intermittency in the presence of noise, *Physical Review E*, 65: 036222.

del Rio, E. and Elaskar, S., New characteristic relation for intermittency type II, *International Journal of Bifurcation and Chaos*, 20 (4): 1185–1191, 2009.

del Río, E. and Elaskar, S., Characteristic Relations and Reinjection Probability Densities (RPD) of Type-II and III Intermittencies. Effect of the noise on RPD. *8th AIMS Conference on Dynamical Systems, Differential Equations and Applications*. University of Technology Dresden , Dresden, Germany, May 25 - 28, 2010.

del Río, E.; Elaskar, S.; Donoso, J. and Conde. L., Noise influence on the Characteristic Relations and Reinjection Probability Densities of type-II and type-III Intermittencies. *3rd Chaos 2010 International Conference*, Chania Crete Greece, 1 - 4 June 2010.

Elaskar, S. and del Río, E., Reinjection Probability Function with Lower Bound of the Reinjection for Intermittency Type III. Mecánica Computacional, 28: 1463-1476 (2009).

Elaskar, S.; del Río, E. and Donoso, J., Reinjection probability density in type-III intermittency, *Physica A*. Submitted.

Kim, Ch.; Known, O.; Lee, E. and Lee, H., New characteristic relations in type-I intermittency, *Physical Review Letters*, 73 (4): 525-528, 1994

Kim, Ch.; Kim, G.; Kim, Y.; Kim, J. and Lee, H., Experimental evidence of characteristic relations of type-I intermittency in an electronic circuit, *Physical Review E*, 56 (3): 2573-2577, 1997.

Kim, M.; Lee, H.; Chil-Min Kim; Hyun-Soo Pang; Eok-Kyun Lee and Known, O., New characteristic relations in Type II and III intermittency, *International Journal of Bifurcation and Chaos*, 7 (4): 831-836, 1997a.

Manneville, P. and Pomeau, Y., Intermittency and the Lorenz model, *Physical Letters A*, 75: 1-2, 1979.

Manneville, P., Intermittency, self-similarity and 1/*f* spectrum in dissipative dynamical systems, *Le Journal de Physique*, 41 (11): 1235-1243, 1980

Pomeau, Y. and Manneville, P., Intermittent transition to turbulence in dissipative dynamical systems, *Communications in Mathematical. Physics*, 74: 189-197, 1980.

Progogine, I., *Las leyes del caos*. Ed. Drakonitos, Barcelona, España, 2009.

Rusband, N., *Chaotic Dynamics of Nonlinear Systems*, John Wiley & Sons, New York, USA, 1990.

Schuster, H and Just, W., *Deterministic Chaos. An Introduction*, WILEY-VCH Verlag GmbH & Co. KGaA, Weinheim, Germany, 2005.

Won-Ho Kye and Chil-Min Kim, Characteristic relations of type-I intermittency in presence of noise, *Physical Review E*, 62 (5): 6304-6307, 2000.

Won-Ho Kye., Sunghwan Rim, Chil-Min Kim, Jong-Han Lee, Jung Wan Ryu, Bok-Sil Yeom. and Young-Jai Park, Experimental observation of characteristic relations of type-III intermittency in the presence of noise in a simple electronic circuit, *Physical Review E*, 68: 036203, 2003.